U.S. DEPARTMENT OF COMMERCE
National Technical Information Service
PB80-100472

Development of an SO2 Monitor for Mobile Sources

Ford Aerospace and Communications Corp, Newport Beach, CA

Prepared for

Environmental Sciences Research Lab, Research Triangle Park, NC

Jul 79

United States
Environmental Protection
Agency

Environmental Sciences Research
Laboratory
Research Triangle Park NC 27711

EPA-600/2-79-121
July 1979

Research and Development

PB80-100472

EPA

Development of an SO_2 Monitor for Mobile Sources

REPRODUCED BY
NATIONAL TECHNICAL
INFORMATION SERVICE
U. S. DEPARTMENT OF COMMERCE
SPRINGFIELD, VA. 22161

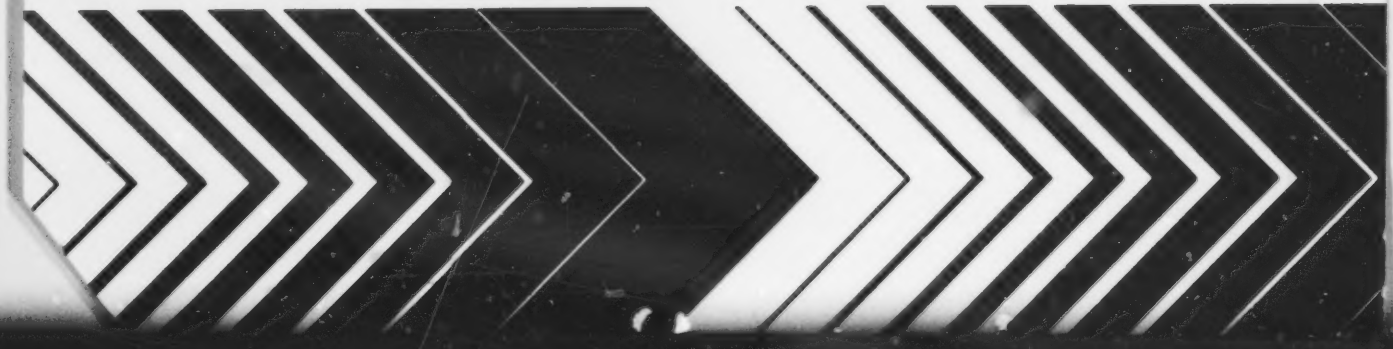

RESEARCH REPORTING SERIES

Research reports of the Office of Research and Development, U S Environmental Protection Agency, have been grouped into nine series These nine broad categories were established to facilitate further development and application of environmental technology Elimination of traditional grouping was consciously planned to foster technology transfer and a maximum interface in related fields The nine series are:

1. Environmental Health Effects Research
2. Environmental Protection Technology
3. Ecological Research
4. Environmental Monitoring
5. Socioeconomic Environmental Studies
6. Scientific and Technical Assessment Reports (STAR)
7. Interagency Energy-Environment Research and Development
8. "Special" Reports
9. Miscellaneous Reports

This report has been assigned to the ENVIRONMENTAL PROTECTION TECHNOLOGY series. This series describes research performed to develop and demonstrate instrumentation, equipment, and methodology to repair or prevent environmental degradation from point and non-point sources of pollution. This work provides the new or improved technology required for the control and treatment of pollution sources to meet environmental quality standards.

This document is available to the public through the National Technical Information Service, Springfield, Virginia 22161.

TECHNICAL REPORT DATA
(Please read Instructions on the reverse before completing)

1. REPORT NO.	2.	3. RECIPIENT'S ACCESSION NO.
EPA-600/2-79-121		

4. TITLE AND SUBTITLE	5. REPORT DATE
DEVELOPMENT OF AN SO_2 MONITOR FOR MOBILE SOURCES	July 1979
	6. PERFORMING ORGANIZATION CODE
7. AUTHOR(S)	8. PERFORMING ORGANIZATION REPORT NO.
D.E. Burch, P.S. Davila, F.J. Gates, and J.D. Pembrook	U-6392
9. PERFORMING ORGANIZATION NAME AND ADDRESS	10. PROGRAM ELEMENT NO.
Ford Aerospace and Communications Corporation Aeronutronic Division Ford Road Newport Beach, California 29663	1AA601B CA-29 (FY-78)
	11. CONTRACT/GRANT NO.
	68-02-2448
12. SPONSORING AGENCY NAME AND ADDRESS	13. TYPE OF REPORT AND PERIOD COVERED
Environmental Sciences Research Laboratory - RTP, NC Office of Research and Development U. S. Environmental Protection Agency Research Triangle Park, North Carolina 27711	Final 10/76 - 1/78
	14. SPONSORING AGENCY CODE
	EPA/600/09

15. SUPPLEMENTARY NOTES

16. ABSTRACT

An instrument has been designed and built to monitor the concentration of SO_2 in the exhaust of mobile sources. A grating assembly desperses the ultraviolet energy from a deuterium-arc source and passes five narrow spectral intervals. Three of the intervals (set A) coincide with strong absorption features in the SO_2 band near 3000 A; the other two intervals (set B) coincide with weak absorption. A spinning reticle alternately transmits energy passing through set A and B to a photomultiplier detector. A dc output signal proportional to the concentration of SO_2 in the sample cell is produced by appropriate electronics.

A pump and manifold assembly permit operation over a wide range of sample flow rates. At high flow rates, the 90% sample turn-over time is approximately 0.7 sec. The sample cell contains a multiple-pass optical system adjusted to 12 passes, giving a sample path length greater than 5 m. The rms noise level corresponds to approximately 0.05 ppm of SO_2 when the electronic time constant is 1 sec.

17. KEY WORDS AND DOCUMENT ANALYSIS

a. DESCRIPTORS	b. IDENTIFIERS/OPEN ENDED TERMS	c. COSATI Field/Group
* Air Pollution * Motor vehicles * Exhaust emissions * Sulfue dioxide * Monitors * Development	Correlation-spectrometer	13B 13F 21B 07B

18. DISTRIBUTION STATEMENT	19. SECURITY CLASS *(This Report)*	21. NO. OF PAGES
RELEASE TO PUBLIC	UNCLASSIFIED	50
	20. SECURITY CLASS *(This page)*	22. PRICE
	UNCLASSIFIED	PCA05/MF A01

EPA Form 2220-1 (Rev. 4-77) PREVIOUS EDITION IS OBSOLETE

EPA-600/2-79-121
July 1979

DEVELOPMENT OF AN SO_2 MONITOR FOR MOBILE SOURCES

by

Darrell E. Burch, Pamela S. Marrs Davila,
Francis J. Gates and John D. Pembrook
Ford Aerospace and Communications Corporation
Aeronutronic Division
Newport Beach, California 92663

Contract No. 68-02-2448

Project Officer

Roy Zweidinger
Emissions Measurement and Characterization Division
Environmental Sciences Research Laboratory
Research Triangle Park, North Carolina 27711

ENVIRONMENTAL SCIENCES RESEARCH LABORATORY
OFFICE OF RESEARCH AND DEVELOPMENT
U. S. ENVIRONMENTAL PROTECTION AGENCY
RESEARCH TRIANGLE PARK, NORTH CAROLINA 27711

DISCLAIMER

This report has been reviewed by the Environmental Sciences Research Laboratory, U.S. Environmental Protection Agency, and approved for publication. Approval does not signify that the contents necessarily reflect the view and policies of the U.S. Environmental Protection Agency, nor does mention of trade names or commercial products constitute endorsement or recommendation for use.

ABSTRACT

An instrument has been designed and built to monitor the concentration of SO_2 in the exhaust of mobile sources. A grating assembly disperses the ultraviolet energy from a deuterium-arc source and passes five narrow spectral intervals. Three of the intervals (set A) coincide with strong absorption features in the SO_2 band near 3000 A; the other two intervals (set B) coincide with weak absorption. A spinning reticle alternately transmits energy passing through set A and B to a photomultiplier detector. A dc output signal proportional to the concentration of SO_2 in the sample cell is produced by appropriate electronics.

A pump and manifold assembly permit operation over a wide range of sample flow rates. At high flow rates, the 90% sample turn-over time is approximately 0.7 sec. The sample cell contains a multiple-pass optical system adjusted to 12 passes, giving a sample path length greater than 5 m. The rms noise level corresponds to approximately 0.05 ppm of SO_2 when the electronic time constant is 1 sec.

This report was submitted in fulfillment of Contract No. 68-02-2448 by Ford Aerospace and Communications Corporation, Aeronutronic Division under the sponsorship of the U.S. Environmental Protection Agency. This report covers the period September 30, 1976 to January 31, 1978, and work was completed as of September 30, 1978.

CONTENTS

Abstract		iii
Figures		v
Abbreviations and Symbols		vi
1.	Introduction	1
2.	Conclusions	3
3.	Recommendations	5
4.	Layout and Optical Diagram	7
5.	Sample Cell	15
6.	Pumps and Manifold	22
7.	Spectroscopic Principles of Detection	26
8.	Electronic Processing of Detector Signal	31
9.	Performance, Calibration, and Discrimination	33

Preceding page blank

FIGURES

Number		Page
1	Photograph of the Optics Assembly, the Manifold Assembly, the Pump Assembly, and the UV Source Power Supply	8
2	Photograph of the Optics Assembly with Front Hinged Panels Closed	9
3	Photograph of the Optics Assembly with Front Hinged Panels Opened	10
4	Optical Diagram of the SO_2 Monitor	11
5	Sectional View of the Sample Cell	17
6	Multiple-Pass Optical System	22
7	Flow Diagram of Pump Assembly	24
8	Flow Diagram of Manifold Assembly	25
9	Spectrum of SO_2 from 2600 to 3300 Angstroms	27
10	Partial Spectrum of SO_2 Band Showing Spectral Slits A and B	28
11	Block Diagram of Signal-Processing Electronics	29

ABBREVIATIONS AND SYMBOLS

AGC	--automatic gain control
cfh	--cubic feet per hour
cfm	--cubic feet per minute
cm	--centimeter
lpm	--liters per minute
m	--meter
ppm	--parts per million by volume
T	--transmittance at a particular wavennumber (or wavelength) that would be measured with a spectrometer having infinite resolving power
T_A	--average transmittance of the absorbing gas (SO_2) in spectral intervals designated by A
T_B	--average transmittance of the absorbing gas (SO_2) in spectral intervals designated by B
V_c	--voltage component of amplified detector signal at carrier frequency, 360 Hz
V_a	--voltage component of amplified detector signal at alternator frequency, 30 Hz
V'	--V_a/V_c, normalized voltage. Normalization is made so that V' = 1 when there is 100% modulation of the beam at 30 Hz

SECTION 1

INTRODUCTION

Most of the sulfur in gasoline is oxidized upon combustion in an engine to SO_2. Concentrations of this gas in raw exhaust are typically between 5 ppm and 50 ppm. At these concentrations, the SO_2 is not considered a serious pollutant unless it is oxidized further to form SO_3, which reacts rapidly with H_2O to form toxic sulfuric acid. Catalytic converters are known to oxidize some of the SO_2 to the more harmful SO_3. Unfortunately, the process by which the SO_2 is converted to SO_3, and ultimately to acid, is difficult to study quantitatively because there is no convenient, real-time method of measuring the acid concentration in the exhaust. It has been found, however, that much can be learned about the behavior of the catalytic converters and about the entire SO_2 conversion process by monitoring the concentration of SO_2 in the exhaust.

The instrument described herein has been designed and built for this purpose, to monitor in real-time the SO_2 concentration in engine exhaust. The low concentration requires that the instrument be quite sensitive and that the discrimination against other exhaust gases be good. Rapid changes in the SO_2 concentration have been observed previously, and it is important that these changes be recorded. This leads to another important requirement, quick response, for the monitor.

The instrument achieves high sensitivity by making use of the very strong SO_2 absorption band near 3000 Å while employing a multiple-pass optical system in the sample cell to obtain a long absorption path in a small volume. An instrument built previously by us[1] for the EPA to monitor SO_2 in stack exhaust made use of the infrared absorption band of SO_2 near 4 μm. This infrared band is too weak to provide the high sensitivity required for the present instrument. Excellent discrimination has been achieved by employing a correlation method that makes use of the structure in the uv absorption band. A low-volume sample cell designed for high gas flow rates used in conjunction with high-capacity pumps makes the quick response possible.

1. Burch, D. E., and D. A. Gryvnak. "Infrared Gas Filter Correlation Instrument for In-Situ Measurement of Gaseous Pollutants." Prepared by Philco-Ford Corporation for EPA under Contract No. 68-02-0575. EPA Report No. EPA-650/2-74-094. Also, Burch, D. E., and D. A. Gryvnak. "Cross-Stack Measurement of Pollutant Concentrations Using Gas-Cell Correlation Spectroscopy." Chapter 10 of Analytical Methods Applied to Air Pollution Measurements, Stevens, R. K. and W. F. Herget, (eds.). Ann Arbor, Ann Arbor Science Publishers Inc., 1974.

The important design goals are summarized as follows:

Sensitivity ranges, full scale: 5, 10, 20, and 100 ppm.

Higher concentrations can be measured by decreasing the number of passes of the multiple-pass cell.

Noise-equivalent-concentration: $\leq$0.05 ppm

Sample turn-over time (90%): $\leq$0.5 sec at maximum flow rate.

Interference by other gases in automotive exhaust should not produce significant error in the SO_2 measurement.

SECTION 2

CONCLUSIONS

It has been demonstrated that an instrument that makes use of the strong SO_2 absorption features near 3000 Å can be designed and built with the sensitivity and accuracy required to measure the concentration of SO_2 in automotive exhaust. Good discrimination against interference by other gases in the exhaust can be achieved by employing the correlation technique used in the instrument described herein. This technique, when used properly, provides very little sensitivity to changes in the reflectivity of mirrors, the transmittance of windows, or variations in source intensity. Electronic circuits developed and used previously by us to process the detector signals of gas-filter correlation instruments work equally well with the present instrument, which employs a grating polychromator with a spinning reticle in place of a gas-filter cell.

The minimum detectable concentration is limited by photoelectron noise generated in the photomultiplier. The noise level measured at the output of the photomultiplier is approximately proportional to the square-root of the radiant energy in the ultraviolet beam incident on the photomultiplier. It follows that increasing the energy level by such means as increasing the source intensity or improving mirror reflectivity would result in an increase in S/N, the signal-to-noise ratio, that is proportional to the square-root of the energy level.

The maximum S/N for a given SO_2 concentration is obtained in the present instrument when the multiple-pass sample cell is adjusted to 12 passes. The necessity for this low number of passes is due to the low effective reflectivity (between 0.80 and 0.85) of the uv-enhanced aluminum coating on the mirrors of the multiple-pass optical system. The actual reflectivity may be higher than this value, but each reflection adds slightly to the distortion of the images. This additional distortion has the effect of lowering the reflectivity by decreasing the amount of energy entering the entrance slit of the grating assembly. Mirrors with a dielectric reflective coating can be made with better reflectivity than the mirrors used near 3000 Å, the spectral region of interest. The reflective coating that is more efficient in the uv was not used because its very low reflectivity in the visible makes it difficult to align the optics with visible light.

Short turn-over times for samples in the sample cell can be achieved by flushing the gas in a low-turbulent stream perpendicular to the monitor beam. If the sample cell is shaped properly and the mirrors and windows are mounted properly, the noise produced on the detector signal by the turbulence is not

significant. Little or no error in sampling is produced by adsorption of SO_2 on the sample cell surfaces because they are coated with non-reactive Kel-F. Teflon coatings adsorbed SO_2 more readily than Kel-F. Anodized aluminum surfaces should not be exposed to SO_2 samples because of the very rapid adsorption.

SECTION 3

RECOMMENDATIONS

The instrument described herein has been designed and built to meet a combination of several desirable specifications as a monitor for SO_2 in mobile sources. Some of the important features are: relatively small size, short response time, variable sample flow rate, very good discrimination, good accuracy, low minimum detectable concentration, and wide dynamic range. Specifications for some of these features necessarily have been sacrificed to improve the specifications of other features. Thus, any SO_2 monitor to be patterned after this one undoubtedly should be modified according to the specific types of measurements to be made with it. A few design changes have become apparent as a result of assembling and testing the present instrument, but even more can be learned by using it for a few weeks under normal testing conditions.

Without changing the basic design, a few relatively minor changes could be made to improve the signal-to-noise ratio by increasing the amount of ultraviolet energy reaching the detector. The biggest gains can be made by employing mirrors with a dielectric reflective coating that has a much higher reflectivity than the uv-enhanced aluminum presently being used. This change, however, would complicate the visual optical alignment because the dielectric mirrors reflect very poorly in the visible. This disadvantage could be overcome by employing mirror mounts that make it possible to remove a mirror and replace it with one of the same radius of curvature without losing optical alignment. Mirror mounts could be adjusted with mirrors having good visible reflectivity; the mirrors then could be replaced with ones having good uv reflectivity. Some of the flat mirrors should be replaced by quartz prisms that are oriented to produce total internal reflection, which can be quite efficient. The prisms should be anti-reflection coated on the surfaces through which the beam passes.

By enlarging the cross-sectional area of the sample cell, the multiple-pass mirrors can be enlarged, thus allowing more energy to be transmitted. The sample cell could be lengthened to increase the electrical signal produced by a given SO_2 concentration. Either of these two changes necessarily increases the sampling volume, which increases either the necessary flow rate or the sample turn-over time, or both. A grating assembly with longer focal length mirrors and/or a larger grating might be required to take full advantage of larger mirrors in the sample cell.

Some gain in signal-to-noise ratio and instability can probably be achieved by replacing the side-looking photomultiplier with an end-looking

one that has a higher quantum efficiency. Stability could also probably be improved by employing a lens between the exit grid and the photomultiplier so that the grating is focused on the photocathode. This would reduce some of the effect of the inherent non-uniform sensitivity of side-looking photocathodes.

The size and complexity of the instrument can be decreased if the specifications are relaxed on either the minimum detectable concentration, the discrimination or the sample turn-over time. As an example, the grating assembly with the grid that produces relatively high spectral resolution could be replaced with a pair of uv interference filters. One filter would transmit a spectral region that includes most of the strong absorption by the entire SO_2 band; the other would transmit an adjacent spectral interval in which the SO_2 absorption is weak. By alternating the filters in the monitoring beam and comparing the transmitted energy levels, the SO_2 concentration could be determined. This simplified method makes use of the absorption by most of the absorption band, but it does not make use of the structure in the band (see Figures 9 and 10), with the result that the discrimination is reduced and the zero-setting of the instrument is more subject to drifts caused by variations in source intensity or by changes in the temperatures of the filters or other optical components.

Gas-filter cells used in conjunction with an interference filter should also be considered as a simpler method. However, gas-filter correlation techniques are not expected to provide discrimination and stability as good as that provided by the grating assembly in the present instrument.

The flow through the sample cell is not as free of mixing as was expected and should be investigated further to determine ways of decreasing the turn-over time. Different shapes for the inside of the sample cell should be tested at typical sample flow rates. The gas flow should be kept parallel to the faces of the multiple-pass mirrors (i.e. perpendicular to the monitoring beam) if high flow rates are required. This avoids excessive turbulence that may be produced by gas flowing around the mirrors.

SECTION 4

LAYOUT AND OPTICAL DIAGRAM

Figure 1 illustrates the pump assembly, the manifold assembly, and the optics assembly. The pump assembly is connected to the manifold assembly with stainless steel tubing, and the manifold is connected to the inlet and outlet of the aluminum sample cell with the same type of tubing. The uv source power supply is also shown in Figure 1. Compressed gas enters the manifold after particulates are removed by a filter mounted on the pump assembly. A wide range of sample gas flow rates is obtainable with the two pumps mounted on the pump assembly and the flow-meters and controls available on the manifold assembly. The gas pressure is indicated at key points in the flow path by pressure gauges. After leaving the manifold, the gas flows into the sample cell and through the sampling volume where the monitoring beam is perpendicular to the direction of the gas flow. The gas absorbs ultraviolet radiant energy from the monitoring beam and then exits from the sample cell. The sample gas is then exhausted through the manifold or passed on to other instruments for further analysis.

Figure 2 is a front view of the optics assembly with the front hinged panels closed and with the available components and controls labeled. Figure 3 is a front view of the optics assembly with the front hinged panels opened and with components and controls labeled appropriately. These figures are discussed in more detail in this section.

Figure 4 is an optical diagram of the SO_2 monitor. Ultraviolet energy from the deuterium arc source is focused by lens L1 onto the field lens L2, which serves as the entrance window of the sample cell. The optical diagram within the sample cell is too complex to illustrate completely for 12 passes of the cell. The distance between mirror C2 and either mirror C1 or C3 is 42.7 cm, giving a 512 cm path for 12 passes. The number of passes can be changed by integral multiples of 4 by use of the adjustment screws located behind mirrors C1 and C3. Mirrors C1, C2, and C3 are bonded to stainless steel back-up plates with the appropriate holes and grooves required for the adjustments.

After passing through the multiple-pass optical system in the sample cell, the beam emerges through the exit window, lens L3. The beam is then incident on flat mirror X1, which is mounted 45° from the vertical. Mirror X1 rotates the beam 90° and directs it downward to flat mirror X2. Mirror X2 is mounted 45° from the vertical, and this mirror rotates the beam 90° and directs it toward spherical mirror X3. Before entering the sample cell, the central ray of the beam is 15.0 cm above the baseplate of the optics assembly.

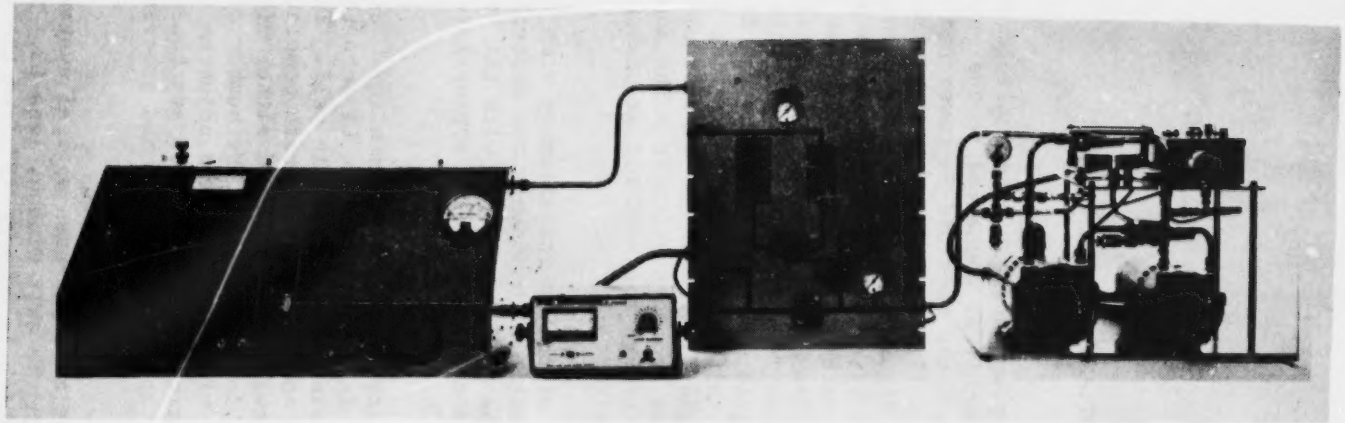

Figure 1. Photograph of the optics assembly, the manifold assembly, the pump assembly, and the UV source power supply.

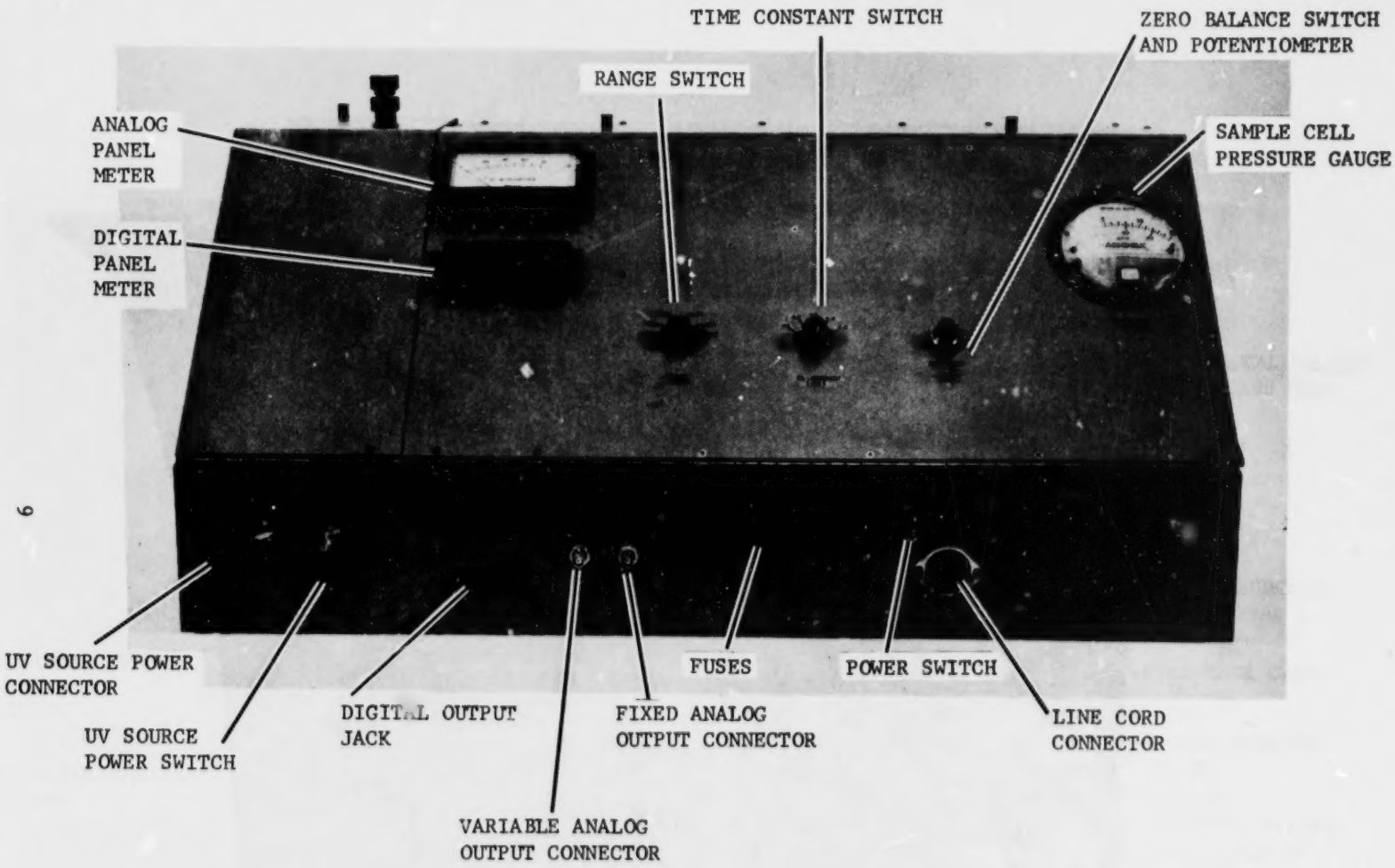

Figure 2. Photograph of the optics assembly with front hinged panels closed.

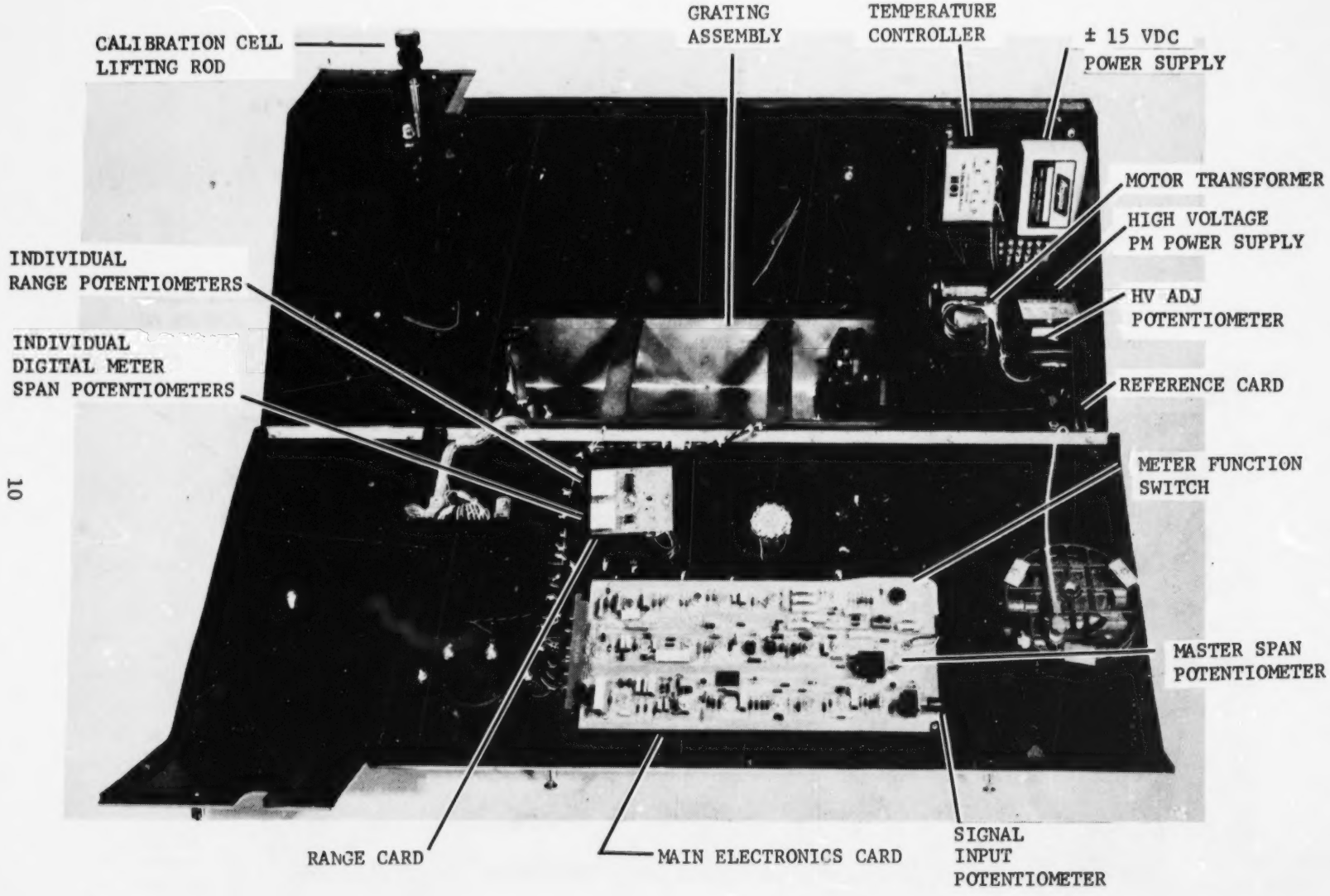

Figure 3. Photograph of the optics assembly with front hinged panels opened.

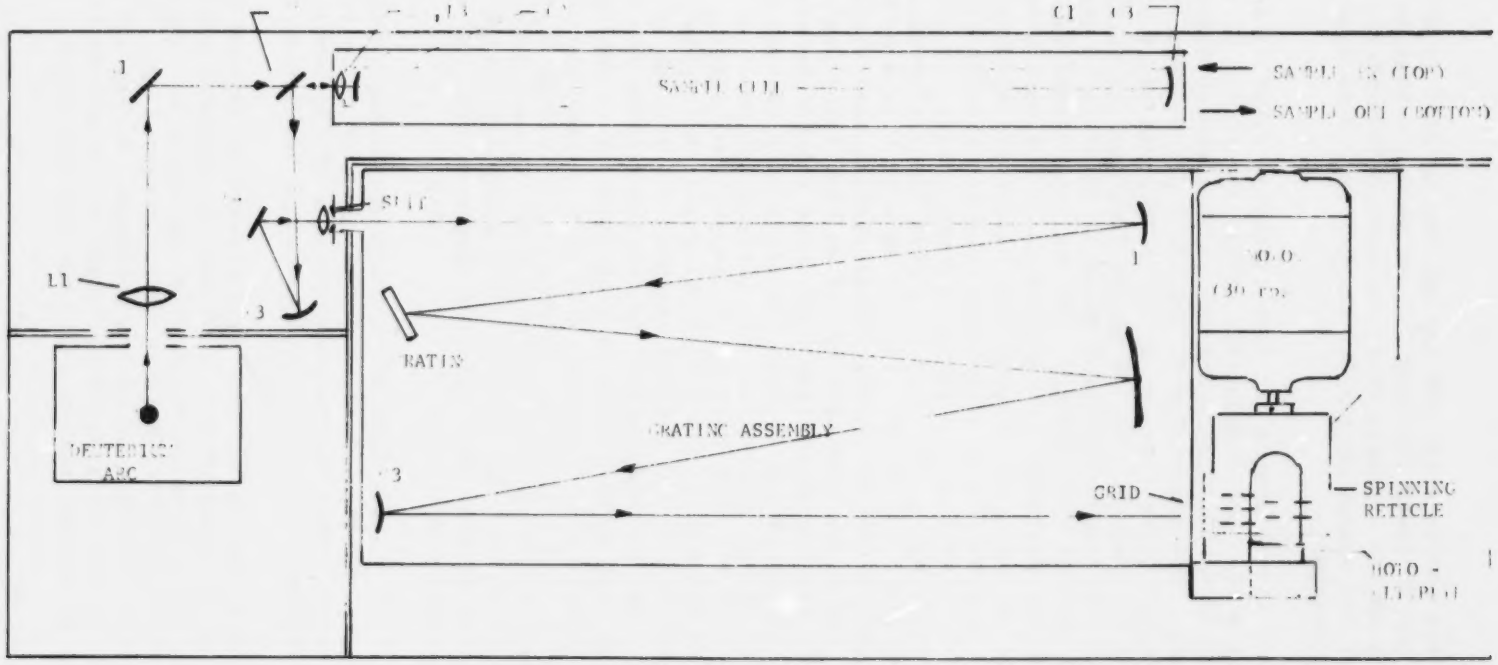

Figure 4. Optical diagram of the SO_2 monitor.

Upon emerging from the sample cell, the central ray is 11.9 cm above the baseplate. Mirrors X1 and X2 lower the beam 5.1 cm; thus the beam is 6.8 cm above the baseplate of the optics assembly after reflection from mirror X2. Mirror X3 forms an image of the source on the 0.3 mm wide by 2.3 mm high entrance slit of the grating assembly.

Spherical mirror G1 collimates the beam of energy after it has passed through the entrance slit. The combination of concave mirror G2 (f = 61 cm) and convex mirror G3 (f = -53.2 cm) focus the radiant energy dispersed by the grating onto the grid. The dispersion at the focal plane where the grid is located is approximately three times as great as it would be if mirrors G2 and G3 were replaced by a single concave mirror identical to mirror G1 (f = 40.6 cm). This increased dispersion makes it possible to use a grid with wider spacings between the openings. In the optical diagram of Figure 4, energy of only a single wavelength is represented in the path from the grating to mirror G2 to the grid. Energy of a wavelength slightly different from the wavelength represented is diffracted from the grating at a slightly different angle and is therefore brought to a focus beside the point of focus of the represented wavelength. The grid is a thin piece of stainless steel shim stock with five slits cut in it. Two 1.5 mm wide by 4.6 mm high slits pass the two B spectral intervals in the SO_2 absorption band where weak absorption occurs. The three 1 mm wide by 4.6 mm high slits pass the three A spectral intervals in the SO_2 absorption band where relatively strong absorption occurs. After passing through the slits, the radiant energy is chopped at 360 Hz, and energy from either the three A intervals or the two B intervals is incident on the CsSb cathode of the photomultiplier, which has a modified S-5 spectral response. The side-looking photomultiplier is supported by a mount attached to the grating assembly and extends into the cylindrical chopper. The photomultiplier is centered inside the cylinder, and the 24 mm wide x 8 mm high photocathode is perpendicular to the beam of radiant energy. A reticle that functions both as a chopper and as a 30 Hz alternator is bonded to the cylindrical chopper. The reticle chops the incoming signal at 360 Hz and also alternately passes the three A intervals, then the two B intervals at 30 Hz. The reticle slits are aligned with the grid slits and are oversized so that this spinning component will not contribute significantly to instabilities, noise, or zero drifts.

The photomultiplier dynode chain has a ten-stage linear configuration. The signal from the photomultiplier is processed electronically to produce a dc output signal proportional to the concentration of SO_2 sample gas. The signal-processing electronics are described in detail in Section 8.

A calibration cell that is filled with a mixture of SO_2 and N_2 can be moved easily into the beam between mirror N1 and the entrance window to the sample cell. The calibration cell is not shown in Figure 4. The optical pathlength through the calibration cell is approximately 4 mm. The cell can be filled to any desired pressure up to 1 atmosphere. Valves and fittings fastened permanently to the calibration cell make it convenient to change the amount of gas in it without removing it from the instrument.

Also not shown in Figure 4, but included with the instrument, is a permanently mounted tungsten-iodide bulb. The tungsten-iodide bulb is mounted

below the beam between lens L1 and mirror N1 and provides visible light to align the optical components in the sample cell and in the grating assembly. The deuterium arc source emits very little visible energy, making it difficult to align optics, particularly after the beam has been reflected a few times. A flat mirror, N2, and a lens, L5, are placed directly above the bulb and in the path of the ultraviolet energy between lens L1 and mirror N1. Thus, from the movable mirror, the beam of visible energy traverses exactly the same path as the ultraviolet energy from the arc source.

A small window on the end of the sample cell opposite the entrance and exit windows makes it possible to view images formed on mirror C2 of the multiple-pass system to determine the number of passes of the monitoring beam. A prism is mounted over the viewing window for viewing the images on mirror C2 from the rear of the optics assembly. The number of passes can be adjusted from outside the sample cell without opening the cell or disturbing the sample.

Figure 2 is a front view of the optics assembly. A digital and an analog panel meter are mounted on the large, front hinged panel. The analog panel meter displays either the dc output signal, the input signal, the reference signal, or the carrier level, depending on the position of the meter function switch mounted on the main electronics card. The dc output signal is always displayed on the digital panel meter regardless of the position of the meter function switch. The analog dc output signal is monitored by connecting a strip-chart recorder to either the fixed or the variable output connector mounted on the lower panel. The output of the fixed output connector is 10 volts for a full-scale reading. The full-scale output of the variable output connector can be adjusted from about 1 millivolt to 10 volts by adjusting a potentiometer and the recorder gain switch on the main electronics card.

The range switch mounted on the front hinged panel is used to select either the 5, 10, 20, 50, or 100 ppm range. When the range switch is in the off position, the dc output of the instrument is zero. The time constant switch is also mounted on the front hinged panel; time constants of 0.1, 0.3, 1.0, 2.0, and 5.0 seconds are available. A 10-turn zero-balance potentiometer and a zero switch are used in combination to electronically cancel any residual 30 Hz modulation on the carrier when SO_2 is not present in the sample gas.

AC power is supplied to the electrical components by connecting a line cord to the "AC IN" male connector and by switching the power switch to the on position. When the power switch is in either the standby or the on position, power is supplied to the heaters bonded to the sample cell and to the power resistors mounted on the sample cell inlet and outlet fittings. After the cell has stabilized at 55°C, the cell can be maintained at this temperature with the power switch in the standby position while other electrical components are inoperative. This feature allows the cell to be maintained at 55°C when tests are not being performed and thus the operator does not have to wait 2 to 3 hours for the cell temperature to stabilize each time before data are taken. The source power switch located on the lower front panel is used to turn the UV source fan on after the UV source power supply

is connected to the source power outlet mounted on the lower front panel. This outlet was installed as a safety feature to prevent the source from being turned on when the cooling fan is not operating.

Figure 3 is a front view of the optics assembly with the front hinged panels open. The main electronics card and the range card are mounted on the inside surface of the front hinged panel. The reference card is mounted on the inside surface of the right side panel. The high-voltage power supply for the photomultiplier, the chopper motor transformer, the $\pm$15 Vdc power supply, and the temperature controller are mounted on the power supply chassis. The chopper motor is mounted on the stainless steel grating assembly and is located below the power supply chassis. The bottom of the sample cell is secured to the baseplate of the optics assembly with two screws. The cell is also secured to the partition that separates the grating assembly from the sample cell. Figure 4 is a top view of the optics assembly showing the locations of the grating assembly, the sample cell, the chopper motor, and the photomultiplier.

Both the sample cell and the grating assembly rest on spacers that hold these two components approximately 1.5 cm above the base plate. The spacers under the sample cell provide insulation to minimize the flow of heat from the sample cell to the base plate. The three spacers under the grating assembly are arranged in such a way as to not put any stress on the grating assembly if the main base plate is distorted slightly.

SECTION 5

SAMPLE CELL

REQUIREMENTS AND GENERAL FEATURES

The two specifications for the instrument that are important factors in the design of the sample cell are the high sensitivity and the quick turnover of gas within the sampling volume. The gas flow through the sampling section may be varied, depending on the type of study being performed. If the concentration of SO_2 in the gas entering the gas line at maximum flow rate changes suddenly from one concentration level A to a second concentration level B, it is desired that the concentration within the sampling volume will have changed 90% of the way from level A to level B within 0.5 seconds after the concentration starts to change within the sampling volume. This exceptionally good time resolution requires a gas flow system with a minimum amount of mixing. The flow rate must be sufficiently high to displace all of the gas in the sampling volume quickly enough to allow for a certain amount of mixing that can not be avoided. Turbulence produced by the high flow rate must not produce significant noise on the signal from the photomultiplier used to detect the monitoring beam.

The second difficult specification calls for the signal-to-noise ratio, S/N to be ≥ 2 for an SO_2 concentration of 0.1 ppm. This high sensitivity requires that the monitoring beam pass through at least a few meters of sample gas. Thus, this imposes certain minimum limits on the size of the sampling volume. This limitation, in turn, requires a relatively high flow rate of the sample gas in order to displace the gas within the sample volume in the required time. The long path of the monitoring beam is obtained by employing a multiple-pass optical system in the sample cell. The sampling volume is made as small as practical while maintaining the mirrors in the multiple-pass optical system large enough to pass an adequate amount of ultraviolet energy through the monitoring system.

CELL CONSTRUCTION AND GAS FLOW

A cross-sectional view of the sample cell is shown in Figure 5. The sample cell is 42.7 cm long in the dimension perpendicular to the plane of the section illustrated. The gas sample enters one end of the distribution tube illustrated in the upper portion of Figure 5. The 1.59 cm I.D. stainless steel distribution tube contains 33 holes evenly spaced in a row in the positions indicated. After leaving the distribution tube through these holes, the gas flows around the distribution tube, through the 0.6 mm throat, and through the cavity in the sample cell perpendicular to the monitoring beam. The cavity in the sample cell is shaped to produce a minimum amount of mixing of the gas before it has passed through the volume traversed by the monitoring beam. After passing the monitoring beam, the gas continues on through another throat 2.3 mm high and enters the collection tube in the lower portion of the sample cell. The gas leaves one end of the collection tube and is either exhausted or passed on to other instruments for further analysis. This type of gas flow produces very little turbulence in the volume traversed by the monitoring beam. At a high gas-flow rate of 200 liters per minute, no additional noise on the detector signal attributable to turbulence can be observed.

The function of the distribution tube is to distribute the gas flow uniformly along the length of the sample cell. Ideally, portions of a small volume of gas that enter the end of the distribution tube at a given time should pass through the holes near one end at the same time that other portions of the same volume element pass through the holes near the middle or near the other end. The mixing and the dwell-time in the distribution tube are reduced to negligible amounts by a tapered piece of rod placed inside the distribution tube, as illustrated in Figure 5. The O.D. of the rod is approximately 0.1 mm less than the I.D. of the distribution tube; the rod is tapered so that the cross-sectional area of the gas volume in the distribution tube decreases in the direction of gas flow.

A few tests were performed with smoke to determine the efficiency of the distribution tube and the mixing inside the sample cell. The ends of the sample cell were replaced with transparent plexiglass so that a laser beam could be passed through the length of the cell at different locations. Light scattered by smoke within the sample cell was observed through the plexiglass end plates. While air was being pumped through the sample cell at a typical flow rate, smoke was injected into the stream of flowing gas just ahead of the inlet to the distribution tube. The smoke could be started or stopped abruptly. As a test of the distribution tube, the laser beam was directed along the cell approximately 1 cm below the throat near the tube, and the air flow was adjusted to between 100 and 150 liters per minute. When the smoke flow was stopped abruptly, the smoke disappeared from the laser beam in less than 0.1 secs, with no distinguishable difference between the times it disappeared from each end. This result indicates that the distribution tube performs its function quite well.

The holes in the collection tube are larger than those in the distribution tube in order to reduce the pressure drop and maintain the absolute pressure in the sampling volume only slightly above the outside air pressure.

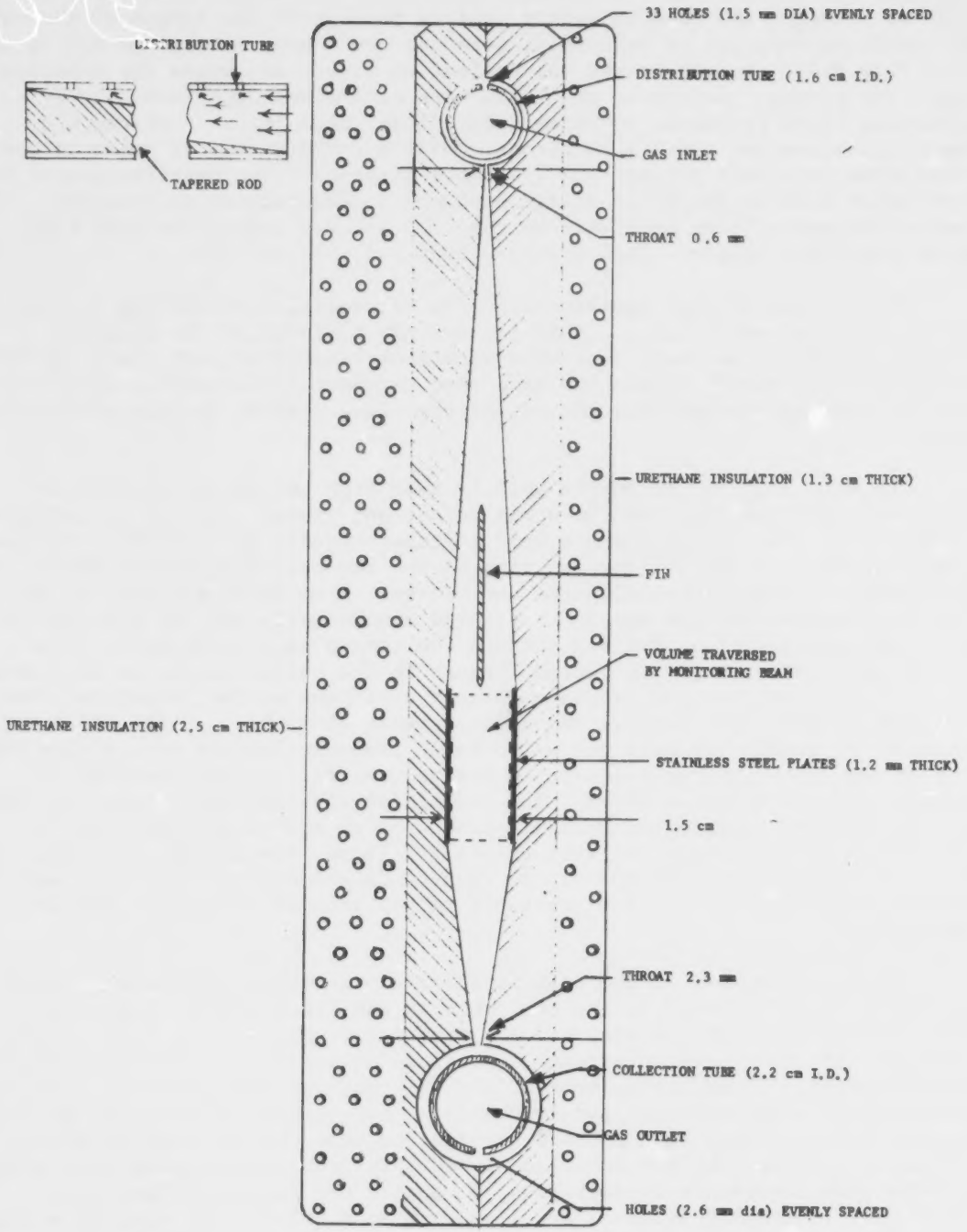

Figure 5. Sectional view of the sample cell. The left-hand portion shows the tapered rod in the distribution tube. The main body of the cell is approximately 31 cm high and 43 cm in the direction parallel to the monitoring beam.

The spacings between the holes were varied along the length of the collection tube so that the gas flow is nearly uniform throughout the length of the cell. If the holes were spaced uniformly, more gas would move across the end of the cell from which the gas leaves the collection tube than across the opposite end. The proper spacings of the holes were determined experimentally by observing light scattered by smoke from a laser beam located between the sampling volume and the 2.3 mm throat. Various combinations of holes in the collection tube were covered and the smoke observed. The distribution of the open holes used in the final design produced a flow-pattern so that the smoke disappeared from both ends of the cell at very nearly the same time after the smoke injected into the airstream had been stopped.

The fin placed just upstream from the monitoring beam divides the gas stream into two equal parts. This fin was not included in the original design, but the flow tests performed with smoke indicated that there was more turbulence and mixing within the cell than had been anticipated. Addition of the fin reduced the apparent mixing and therefore reduced the gas turn-over time.

The main body of the sample cell is made from two nearly symmetrical pieces of aluminum that have been milled out and placed together as indicated in Figure 5. The two pieces are held together rigidly by 12 bolts. Silicone rubber provides a seal at the junction of the two main side pieces and at the junctions of these pieces with the end plates. A vacuum-tight seal is not required because the gas sample is flushed continuously and the pressure is very near atmospheric. The pressure in the sample cell is slightly above atmospheric when the gas is pumped through in the normal manner as discussed in Section 6. If the gas is drawn through by a pump on the downstream side of the sample cell, the pressure is slightly below atmospheric. The difference between the sample pressure and atmospheric pressure depends on the flow rate and on the amount of constriction by the valves, filter, etc. between the sample cell and the atmosphere. The end plates for the sample cell, not shown in the figures, support the multiple-pass optical system and the windows through which the monitoring beam enters and leaves the sample cell. Gas fittings also mounted to the end plates connect to the distribution tube and the collection tube so that these two tubes can be removed easily and cleaned, if necessary.

The aluminum body of the cell is anodized to prevent corrosion. Sensitivity tests performed with the cell when it was first assembled indicated that the anodized surface adsorbed SO_2 from dilute mixtures at such a rapid rate that it would produce erroneous readings unless the gas flow was exceptionally high. In addition, some of the SO_2 that had been adsorbed previously would desorb from the walls and contaminate "zero-gases" or mixtures of lower concentration as they were flushed through the cell. After testing several different coatings for the anodized aluminim to reduce adsorption while maintaining good resistance to corrosion, we coated the inside surface with KEL-F 800. The solid material was dissolved in a solvent and sprayed on the anodized surface and heated for a total of about 5 hours at different temperatures up to 425°F. Tests indicate that the rate of adsorption of SO_2 on this material is slow enough that it can be accounted for by slowly flushing the sample through the cell.

The two thin stainless steel plates on either side of the volume traversed by the monitoring beam were added after the aluminum sides were made and some preliminary tests were performed. These plates reduce the width of the gas stream, decreasing the amount of mixing and, in turn, reducing the gas turnover time. The surfaces of these plates were roughened by sandblasting to reduce the specular reflection of light from the surfaces on which "spill-over" of the monitoring beam is incident. Extra light from the oversize monitoring beam is incident on these surfaces at a grazing angle, causing the reflection to be quite efficient. The reflected light is a possible source of error because it does not travel the same distance in the sample as does the main beam. In addition, this reflected light makes alignment of the multiple-pass optics confusing. No Kel-F coating was put on these stainless steel plates because it would form a glossy surface and reduce the effect of sandblasting. No coating on stainless steel is required because the adsorption of SO_2 on this metal is negligible.

CELL HEATING

Condensation of water in the sample cell is avoided by heating the cell to any desired temperature up to approximately 60°C. Electrical heating tapes, not shown in Figure 5, are bonded to the sides of the cell and provide the heat. Heating wires attached to the inlet and outlet gas lines provide additional heat to these parts. A temperature sensor embedded in the side of the cell near the monitoring beam provides the input signal to a controller that varies the power to the heater as required to maintain a constant temperature. The temperature to which the cell is regulated is varied by adjusting a small potentiometer on the temperature controller. When the instrument was delivered to EPA, the temperature controller was adjusted to approximately 55°C, which is high enough to avoid condensation under most operating conditions even if some parts of the cell are a few degrees cooler than the part near the sensor. A transformer in the heater circuit limits the maximum voltage across the heaters to 36 volts. During typical operation, the duty cycle of the heater is between 20% and 40%. Approximately 2 hours are required to bring the cell from room temperature to 55°C.

Two thermocouples make it convenient to monitor temperatures with a high input-impedance voltmeter. One of the thermocouples is embedded in the aluminum side of the cell adjacent to the sensor for the controller. This makes it possible to determine the control temperature and to monitor the performance of the controller. The other thermocouple extends through the side of the cell wall into the gas at a point just downstream from the monitoring beam. This thermocouple monitors the gas temperature, which may fluctuate and differ by a few degrees centigrade from the cell walls. The two thermocouples are made of iron and constantan wires; the emf produced is 0.052 mv for each °C difference between the sensing junction and the reference junction of the thermocouple.

Sheets of urethane insulation approximately 1.5 cm thick insulate the main cell body. Four stainless steel posts, each approximately 1.2 cm long and 1.2 cm in diameter support the cell body and insulate it thermally from the remainder of the optics assembly. A solid aluminum partition (see Figure 4) separates the sample cell from the grating assembly and the electronics. During typical operation, the grating assembly and the electronics are less than 5°C above room temperature.

OPTICAL COMPONENTS OF SAMPLE CELL

Figure 6 illustrates the optical portions of the sample cell. A side view of the multiple-pass optical system is shown in the upper panel. Mirrors C1, C2, and C3 are nearly flush with the inside surfaces of the endplates so that they interfere a minimum amount with the gas flow. An image of the deuterium arc source is formed beside mirror C2 and just inside lens L2, which also serves as a window. Spherical mirrors C1, C2, and C3 have a common radius of curvature that is equal to the distance from mirror C2 to C1 or C3. Images are formed on mirror C2 as indicated in the lower panel of Figure 6 when the optics are adjusted for 12 passes. The image pattern is viewed through the window below mirror C3. The number of passes is changed by adjusting mirror C3. When adjusting the optics, the tungsten-iodide bulb is used as an energy source because it emits much more visible energy than the arc. The centers of lenses L1 and L2 are separated by approximately 30 mm, and the openings in the endplates near these lenses are approximately 5 mm in the long dimension. Mirrors C1 and C2 are each 16 mm square. Thus the cross section of the volume of gas being monitored is approximately 16 mm by 32 mm.

The oblong opening in the endplate near lens L2 is overfilled by the enlarged image of the deuterium arc source. Therefore, the images on mirror C2 have the shape of the oblong opening in the endplate. Lens L2 forms an image of lens L1 near mirror C1. Lens L3 images mirror C3 near spherical mirror X3 (see Figure 4). Flat mirrors X1 and X2 are each tilted approximately 45° from the vertical. The combination of these two mirrors lowers the beam and directs it horizontally to mirror X3, which forms an image on the entrance slit of the grating assembly. The image formed at lens L3 is rotated 90° by mirrors X1 and X3 with the result that the long dimension of the image at the entrance slit is parallel to the length of the slit. The entrance slit, 0.3 mm wide by 1.5 mm high, is over-filled in width and slightly under-filled in height.

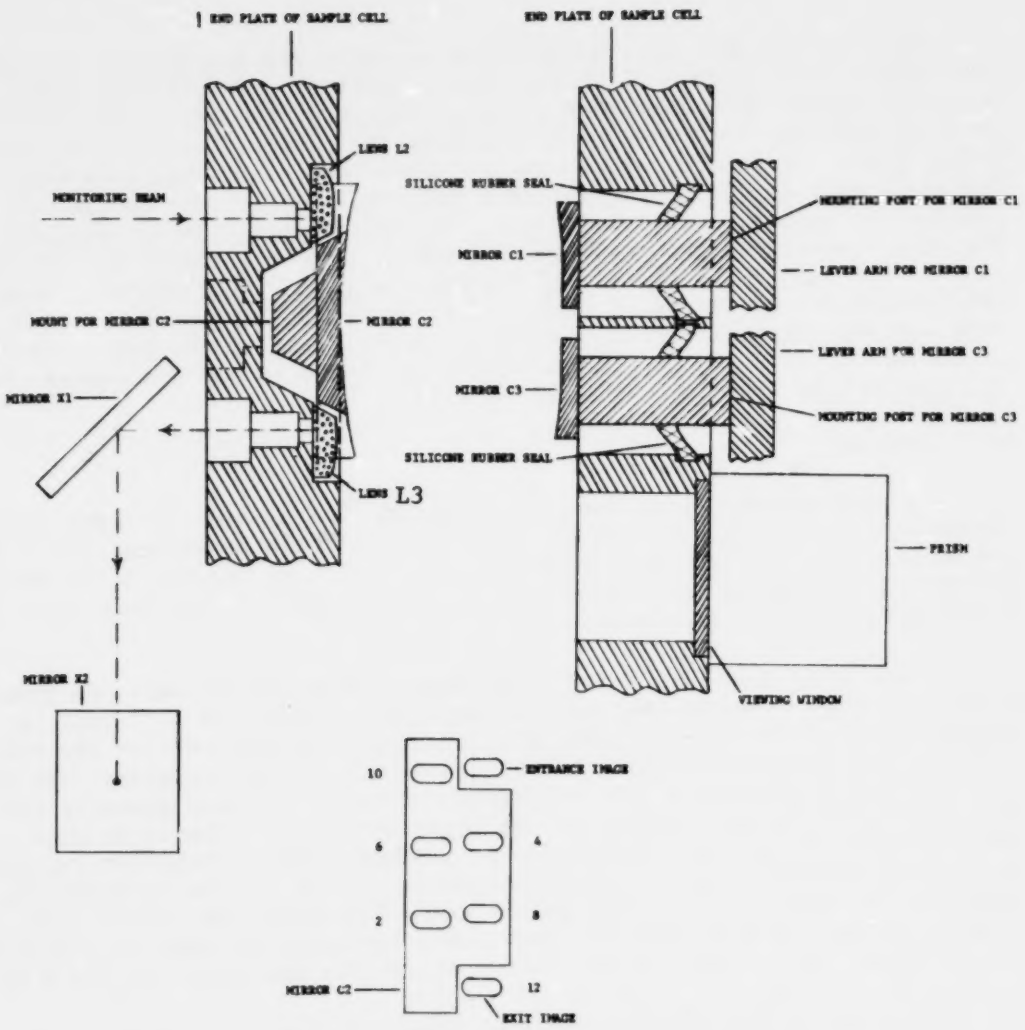

Figure 6. Multiple-pass optical system. The cross-sectional views illustrate the manner in which the optical components are assembled. The image pattern on mirror C2 is shown in the lower panel.

SECTION 6

PUMP AND MANIFOLD ASSEMBLIES

The pump assembly and the manifold assembly are designed to provide the user with a wide variety of sample flow conditions. Sample flow rates can be varied easily from less than 5 lpm to more than 160 lpm. Flow rates are adjusted with the manifold assembly and by the choice of one of two pumps. During normal operation, sample gas is drawn into the system to a pump that forces it through the manifold system and sample cell. The sample cell pressure is slightly more than 1 atm. By re-arranging some of the gas-handling components, the pumps can be made to draw the sample gas through the sample cell before the gas passes through the pump or the manifold assembly. This latter procedure may be useful if it is found that the pump or the manifold assembly changes the concentration of SO_2. All of the following discussion pertains to normal operation during which the sample gas passes through the pump before it reaches the sample cell.

PUMP ASSEMBLY

The pump assembly with two pumps mounted side-by-side is represented schematically in Figure 7. Sample flow rates as high as approximately 160 lpm can be achieved with the high-capacity pump if all of the gas lines are short and have sufficiently large diameters. Approximately 80 lpm flow rate can be achieved with the smaller pump.

A three-way electric switch is mounted on the pump assembly so that either the high-capacity pump or the low-capacity pump can be turned on. The operator must check several valve positions and settings on both the pump assembly and the manifold assembly before turning on either pump. Two three-way ball valves mounted on the plexiglass front of the pump assembly are used to switch the gas lines. If the high-capacity pump is to be used, these two three-way valves must be rotated to the high-flow position so the gas can pass from the pump to the manifold assembly. Valves on the manifold assembly must also be opened to pass the sample gas. Similarly, the valves must be rotated to the low-flow position before the low-capacity pump is turned on. The three-way valves and the electrical switch for the pumps are color-coded.

Connected to the line leaving each pump are a pressure gauge, a pressure switch and a pressure-relief valve. The pressure gauge is useful in monitoring the output pressure of the pump which must be kept below 10 psig to avoid damaging the pump. The adjustable pressure switch automatically turns off the electrical power to the pump when the pressure exceeds approximately 9 psig. The pressure-relief valve opens at about the same pressure and serves as an additional safety feature.

Compression of the sample gas by the pumps heats the gas, making additional heating of the outlet lines unnecessary. The amount of heating increases with increasing pressure in the outlet line. When the high-capacity pump is operating with 8 psig pressure, the outlet line may reach a temperature as high as 85°C.

MANIFOLD ASSEMBLY

The manifold assembly, shown schematically in Figure 8, makes it possible to adjust the rate of flow of the sample gas to the desired level. Low-flow rates are read from a small flow meter with a full-scale reading of 80 standard cfh (38 lpm). A larger flow meter with a full-scale reading of 6 cfm (170 lpm) measures higher flow rates. A 3-way ball valve is used to direct the gas through the appropriate meter. The drop in pressure from the outlet of the manifold to the sample cell can be determined by comparing the pressures indicated by the gauges at these two locations.

Both the flow-adjust valve and the bypass valve are used simultaneously to adjust flow rates. Opening the bypass valve prevents the pressure from building up to a high level when the flow-adjust valve is adjusted for a low flow rate. Approximate pump pressures can be determined easily from the gauge near the inlet to the manifold.

Calibration gas is flushed through the manifold to the sample cell by opening a toggle valve in the calibration-gas line. A standard fitting on the end of the calibration-gas line makes it easy to connect it to a container of gas mixture with a known concentration of SO_2. The flow-adjust valve is closed when calibration gas is introduced into the sample cell.

The flow meters, gauges, valves and gas lines on the manifold assembly are heated to approximately 55°C to avoid condensation of H_2O. A 36 -volt transformer provides electrical power, at a safe voltage, for the heating wire wrapped around all of the components that are in direct contact with the sample gas. A contact switch attached to the gas line opens, stopping the electric current, when the temperature reaches approximately 55°C. A small light indicates when electrical power is being supplied to the heating wire. The switch-point can be adjusted to other temperatures. All of the heated components are packed in insulation and enclosed in a metal box. Handles for the valves extend through the front panel of the box. Glass windows on the front panel make it possible to see the scales on the gauges and flow meters.

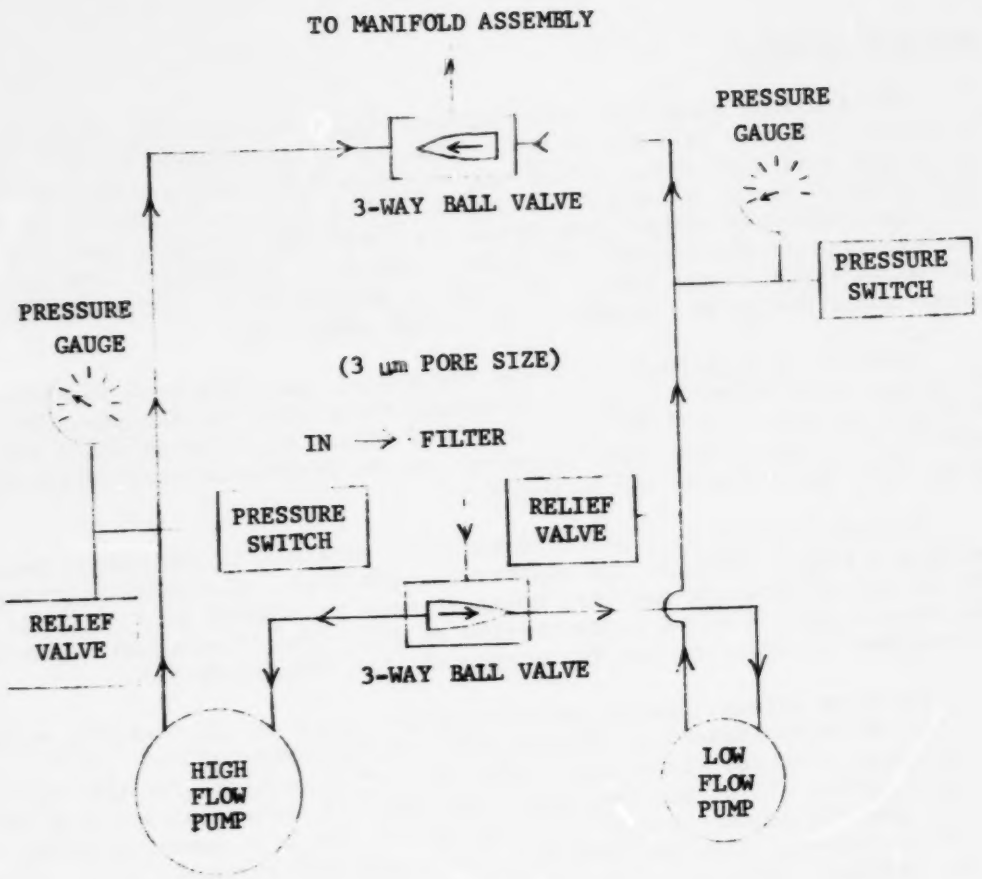

Figure 7. Flow diagram of pump assembly.

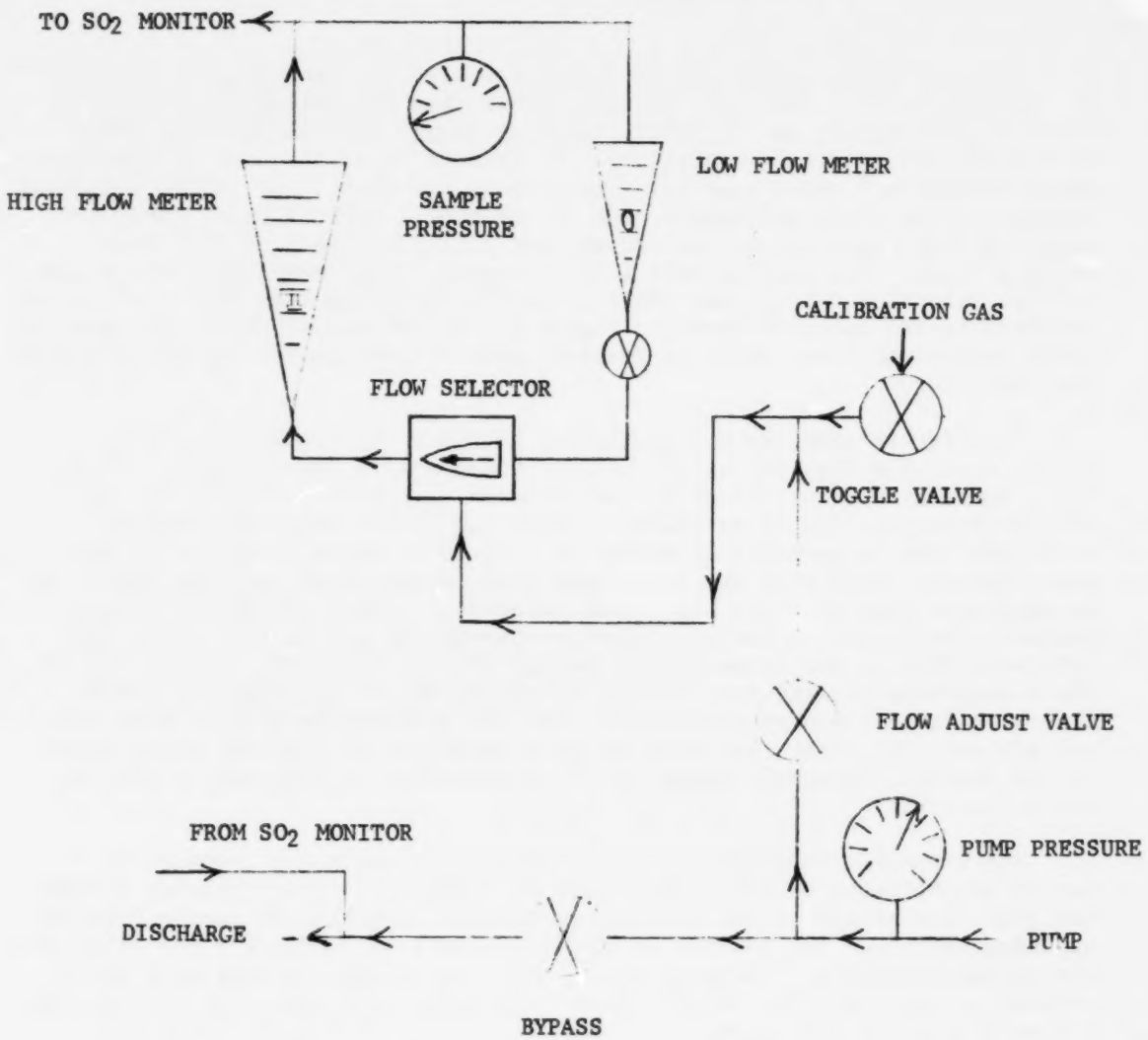

Figure 8. Flow diagram of manifold assembly.

SECTION 7

SPECTROSCOPIC PRINCIPLES OF DETECTION

Figure 9 shows a spectrum of the ultraviolet SO_2 band that is employed by the instrument. This band is used rather than the well-known 4 μm band, which is much weaker and therefore requires longer optical paths in order to achieve the required sensitivity. It is noted that the part of the band shown in Figure 9 shows some relatively sharp structure, but little structure appears on the short wavelength side of the band. Each of these structural features that stand out in the region near 3000 Å consists of many overlapping lines. For samples near 1 atm pressure, these many lines are broadened so that they overlap and there is little remaining structure that is not resolved in the spectrum shown in Figure 9. At low sample pressures, many of these individual lines could be resolved with a spectrometer having very high resolving power.

In order to simplify the problem of handling the sample gas, it is highly desirable that the sample be maintained near 1 atm pressure. Therefore, the very fine structure in the spectrum cannot be exploited for detection purposes. It is necessary to make use of the relatively coarse structure that is observed in Figure 9. Figure 10 shows a portion of the spectrum near 3000Å with the wavelength scale expanded so that the lines can be seen more clearly. The instrument makes use of this relatively coarse structure by comparing the transmission through the gas in the 3 intervals labeled with A to the transmission through the two intervals labeled with B. The A intervals include very strong absorption by the SO_2, whereas the B intervals contain weaker absorption. The two B intervals are the same width and are each 50% wider than each of the A intervals so that the total width of the spectral intervals passed by the B intervals is the same as that by the A intervals.

The average transmissions through intervals A and B are compared by use of the spinning reticle illustrated in Figure 11. After passing through the grid, the energy of the selected wavelength intervals is incident on the spinning reticle. The reticle is bonded around a cylindrical piece of aluminum tubing which has 12 equally spaced slots cut along its long axis and is secured to the shaft of a motor, which rotates at 1800 rpm. The reticle has 6 rows of 3 slits and 6 rows of 2 slits cut in it. The three slits are aligned directly behind the three grid openings that correspond to slit intervals A. The two slits are aligned directly behind the grid openings that pass intervals B. The openings in the reticle are oversized with respect to the grid openings so that this spinning component will not contribute significantly to instabilities, noise, or zero drift in the output signal. The

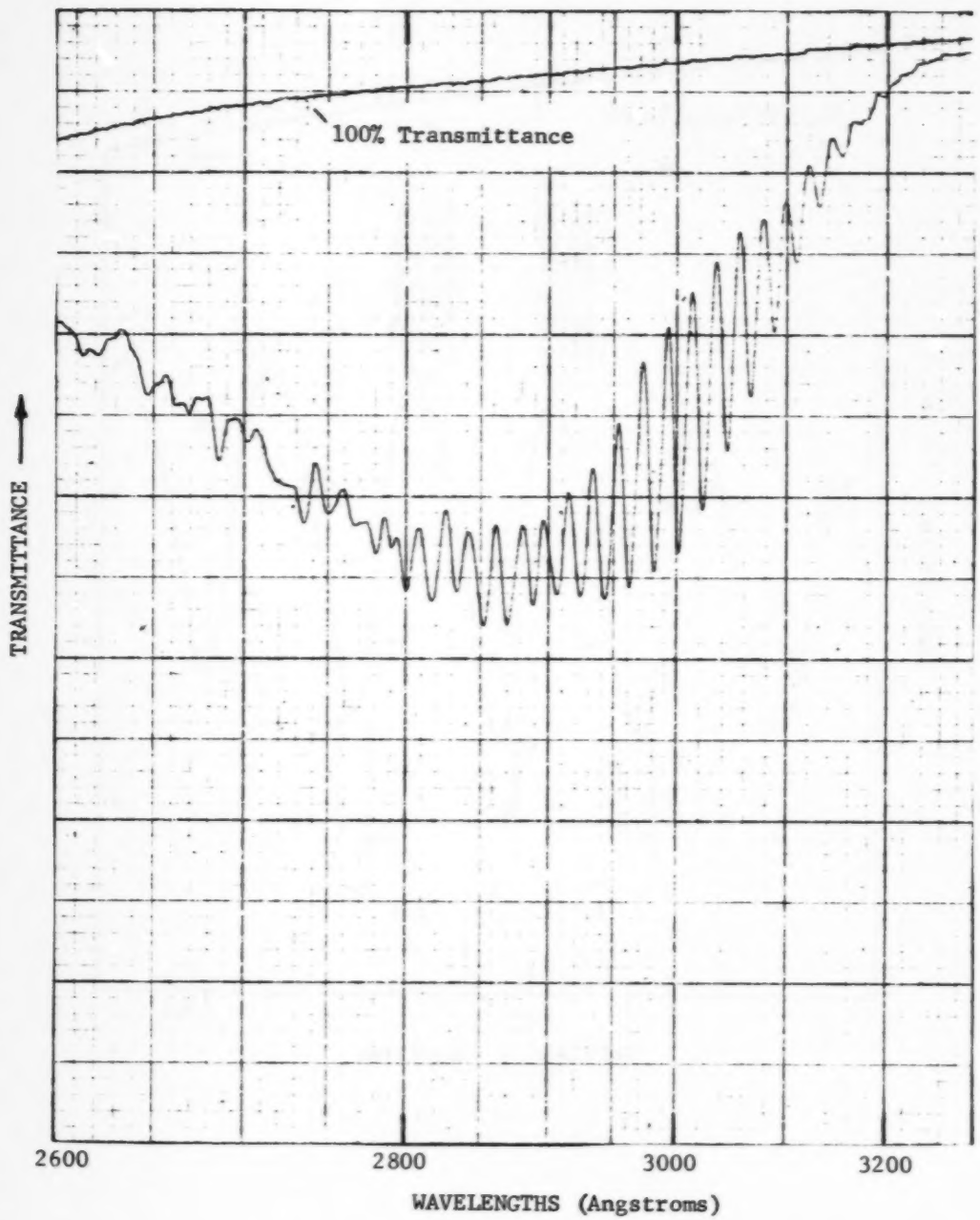

Figure 9 . Spectrum of SO_2 from 2600 to 3300 Angstroms. The sample consisted of 0.1 atm of pure SO_2 in a 0.4 cm cell.

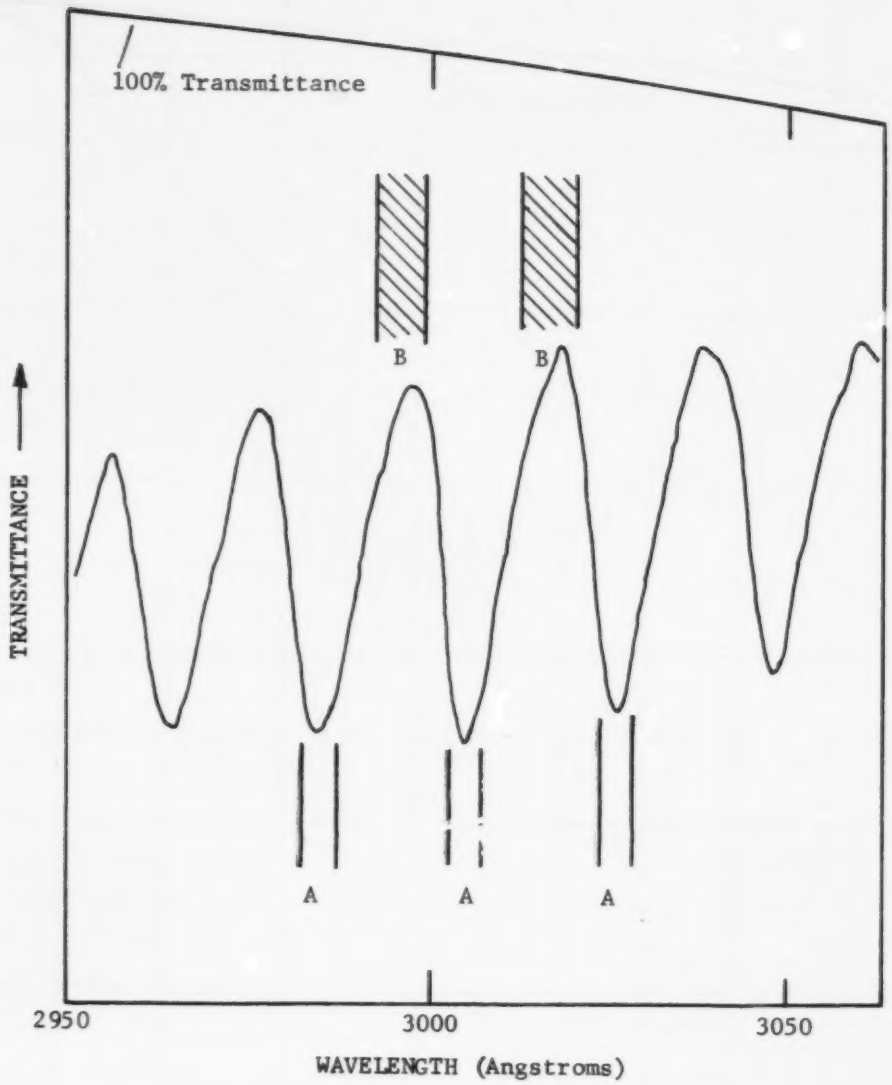

Figure 10 . Partial spectrum of SO_2 band showing spectral slits A and B.

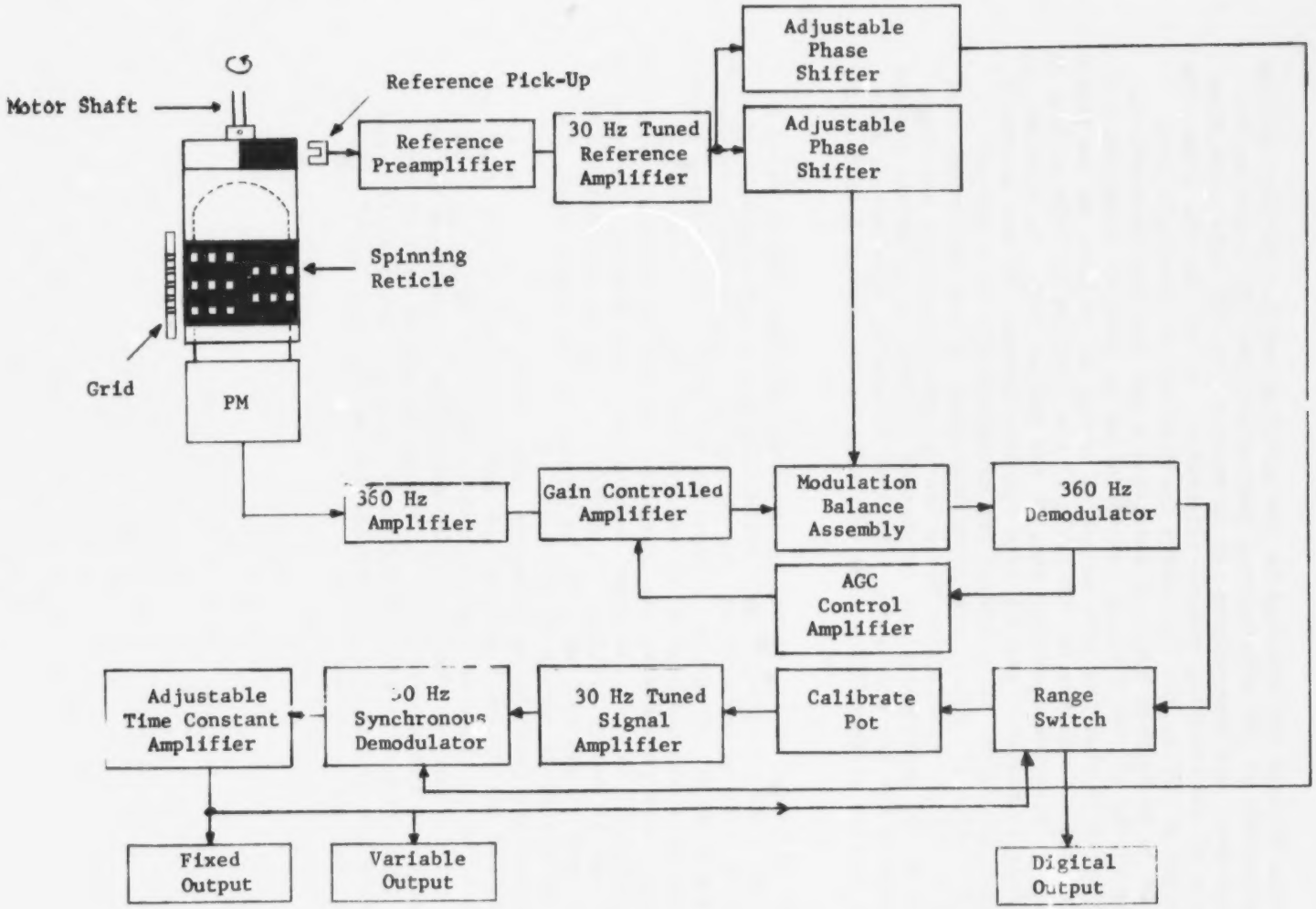

Figure 11 . Block diagram of signal-processing electronics.

energy passing through the openings in the spinning reticle travels radially to the photocathode of the side-looking photomultiplier, which has an S-5 spectral response. The photomultiplier is mounted with its axis coincident with the axis of the rotating chopper-alternator. As the reticle spins, the beam is chopped at 360 Hz and the energy incident on the photomultiplier alternates at 30 Hz between spectral intervals A and spectral intervals B. The relative widths of the openings corresponding to spectral intervals A and B is adjusted so that the same amount of energy is incident on the photomultiplier during both halves of the cycle of the spinning reticle as long as there is no SO_2, or other absorbing gas, in the sample cell. In practice, it is not possible to maintain exactly this equality between the two intervals, but the slight imbalance is accounted for electronically by a method described in Section 8. After some experimentation, it was determined that the cathode of the photomultiplier has a non-uniform sensitivity and thus the response of the photomultiplier to photons incident on different regions of the cathode is not the same. The imbalance created by this non-uniform sensitivity is also accounted for electronically by the method described in Section 8.

A 30 Hz component of the detector signal results when SO_2 is added to the sample cell, and the size of this signal depends on the source brightness, amount of dirt on the windows, and on any other parameters that might change the total amount of energy incident on the slit of the grating assembly. In order to avoid the problem of the detector output signal being dependent upon these parameters, the instrument is made to measure a quantity that is proportional to the fractional modulation of the beam, rather than to the total change in energy striking the detector. This is accomplished by chopping the beam at 360 Hz. When SO_2 is present in the sample cell, the 360 Hz carrier signal is modulated at 30 Hz. The carrier signal is maintained at a constant level by an automatic gain control circuit. The electronics described in Section 8 process the detector signal in such a way as to produce a dc output that is proportional to $(T_B - T_A)/(T_B + T_A)$. This quantity is proportional to the fractional modulation of the beam and is related directly to the concentration of SO_2 in the sample cell of fixed pathlength. The changes in source brightness, detector responsivity, and electronic gain are automatically accounted for so that the "span" calibration remains constant.

SECTION 8

ELECTRONIC PROCESSING OF DETECTOR SIGNAL

Figure 11 is a block diagram of the electronics that process the signal from the detector and produce a dc voltage that is proportional to the concentration of SO_2. The relationship between the output voltage and the gas concentration is determined by calibrating the instrument with samples of known concentration. The electronics consist basically of two demodulators in series. The first demodulator operates at 360 Hz, the carrier frequency determined by the chopper. The average dc component in the output from the first demodulator is proportional to the amount of radiant energy chopped by the spinning reticle. The 30 Hz component of the signal output of the first demodulator is proportional to the modulation of the beam at this frequency. This 30 Hz component then passes through a series of gain controls and amplifiers to the second demodulator, which is synchronous and receives its reference signal from a reference pick-up mounted near the rotating grid chopper. The output of the second demodulator is then proportional to the 30 Hz modulation, and thus to the concentration of SO_2 in the sample cell.

The amplified component of the detector signal at the carrier frequency, 360 Hz, is defined to be V_c. Correspondingly, the component at the modulation frequency, 30 Hz, is defined as V_a. It is desirable for the instrument output to be proportional to the fractional modulation of the carrier signal. This fractional modulation is proportional to V_a/V_c, which we define as V', and it is desired that this relationship be independent of source brightness, detector sensitivity, etc. An automatic gain control (AGC) circuit maintains V_c at a constant value. If, for example, the signal from the detector decreases because of dirt on the windows or a decrease in source brightness, the gain of the gain-controlled amplifier increases to maintain V_c constant. The increase in gain also increases the amplification of both the 360 Hz carrier signal and the 30 Hz modulation signal by the same factor. Therefore, V' is kept directly proportional to the output V_a and maintains a constant relationship with the gas concentration. The AGC circuit can account for changes in the 360 Hz component of the signal by approximately a factor of 4.

The reference pick-up for the 30 Hz synchronous demodulator consists of a light-emitting diode (LED) and a small phototransistor. The phototransistor senses the light reflected from the metallic tape wrapped around the outside of the spinning reticle.

A zero-balance assembly electronically accounts for any imbalance between the two beams passing through spectral intervals A and spectral intervals B when there is no absorbing gas in the sample cell. This

electronic assembly would not be required if it were practical to obtain a perfect optical balance between the two sets of slit intervals and if the cathode of the photomultiplier had a uniform sensitivity. Approximately a $\pm$ 10% variation in the transmittance through either of the sets of intervals can be accounted for by this electronic zero-balance assembly. The assembly changes the amplification ahead of the 360 Hz demodulator during the two halves of the cycle of the spinning reticle. The signal from the 30 Hz reference pick-up switches the zero-balance assembly between the two different gains with the proper phase. The difference in the gains between the two halves is adjustable by the "zero" potentiometer mounted on the front panel of the instrument.

Five ranges of sensitivity are provided; 5, 10, 20, 50, and 100 ppm. The gain in each range can be adjusted independently over a factor of approximately 4. A six-position switch mounted on the front hinged panel of the optics assembly makes it convenient to change ranges. When the switch is in the off position, the output of the 360 Hz synchronous demodulator is shorted to ground. Because of optical saturation, it is necessary to reduce the number of passes to 2 or 4 passes in order to operate in the 0 - 1000 ppm range. All ranges must be recalibrated with appropriate span gases for operation in the 0-1000 ppm range.

A four-position switch mounted on the main electronics card makes it possible to use the analog panel meter to monitor other quantities in addition to the signal output. With the switch in one position, the meter indicates the level of the reference signal; with the switch in another position, the meter reads the level of the 360 Hz signal from the photomultiplier before the automatic gain control circuit; with the switch in still another position, the meter indicates the signal input level. Thus it is possible to check to see that both the reference signal and the carrier level are within the correct operating range.

The digital panel meter directly indicates the SO_2 concentration in the sample gas. The relationship between the analog meter indication and the concentration, of course, depends on the range to which the instrument is set. The digital panel-meter is connected to an output jack so that the digital output can be recorded or transmitted over a line to another instrument. The size of the analog voltage output that corresponds to full-scale reading of the instrument can be varied continuously from less than 1 mV to 10 V. Thus, this analog output can be recorded easily with virtually any strip-chart recorder with a high input impedance.

SECTION 9

CALIBRATION AND PERFORMANCE

SPAN CALIBRATION

Each of the five sensitivity ranges (5, 10, 20, 50, and 100 ppm full-scale) has been calibrated with the sample cell controlled at 55°C. The calibration depends on the cell temperature because the instrument response is approximately proportional to the number density of SO_2 molecules, regardless of temperature. If the SO_2 concentration in ppm remains constant and the pressure is one atm, an increase in temperature results in a proportional decrease in the number density of SO_2 molecules in the monitoring beam. Thus, the instrument response decreases and the potentiometers used to vary the gains of the electronic circuits must be adjusted so the meters will indicate the proper concentration. In most cases, a small correction to the calibration for all five ranges can be made by adjusting a single potentiometer that changes the gains for all five ranges by the same factor.

At a fixed temperature, the output signal is essentially proportional to SO_2 concentration for concentrations less than 30 ppm. At higher concentrations, the response becomes slightly non-linear, necessitating small corrections. The meters and the voltages on the output jacks are directly proportional to the output signal; no circuits have been added to account for the non-linearity. Table 1 contains the information required to correct for the non-linear response when using the 50 ppm and 100 ppm full-scale ranges. No correction is required for the 5, 10, and 20 ppm full-scale ranges.

TABLE 1. CORRECTIONS TO CALIBRATION TO ACCOUNT FOR NON-LINEAR OUTPUT

Meter Reading (ppm)	Correction (%)	Corrected Reading (ppm)
	50 ppm Full-Scale Range	
≤ 30	0	Same as meter
40	+1	40.4
50	+2	51.0
	100 ppm Full-Scale Range	
≤ 30	-4	0.96 x meter reading
40	-3	38.8
50	-2	49.0
60	-1	59.4
70	0	70.0
80	+1	80.8
90	+2	91.8
100	+3	103.

Errors due to the non-linear relationship between SO_2 concentration and output signal are negligible for the 5, 10 and 20 ppm full-scale ranges, and for concentrations lower than 30 ppm measured on the 50 ppm full-scale range. The approximate corrections required for the 50 ppm and 100 ppm full-scale ranges are given above. The gain for the 100 ppm full-scale range has been adjusted so that it is nearly correct at 70 ppm. Thus the maximum error due to non-linearity on the 100 ppm full-scale range is approximately 3% for any sample that would normally be measured on this range.

The same corrections apply whether the values are read from the analog panel meter, the digital panel meter, or one of the output jacks.

ADSORPTION OF SO_2 ON CELL WALLS

Sulfur dioxide adsorbs readily to the walls of containers. The adsorption process may take place for several minutes before the amount adsorbed on the walls comes to an equilibrium. The equilibrium amount depends on the concentration of the SO_2 vapor in contact with the walls. The SO_2 monitor senses only the concentration of SO_2 in the vapor phase; therefore sizeable errors can be made if adsorption is ignored or not accounted for properly. In order to minimize the problem due to adsorption, we have coated the inside surface of the sample cell with Kel-F 800, an inert plastic material that is noted for low adsorptivity. Nevertheless, some care in sampling is still required because of adsorption in the gas lines and the small amount that occurs in the sample cell.

The simplest method of accounting for the adsorption is to flush the gas sample continuously through the sample cell so that the SO_2 that adsorbs on the walls is replenished before the vapor concentration is depleted significantly. "Zero" gas being used when adjusting the zero-setting should also be flushed to carry away SO_2 that comes off the cell wall after having been adsorbed from previous samples.

A few simple tests were performed to determine the rates of adsorption and the rate of sample flow required to avoid significant errors in the measurements. The first test involved introducing a sample of 3.9 ppm SO_2 concentration into the sample cell after it had been flushed with N_2 long enough that there was essentially no SO_2 adsorbed on the walls. The 3.9 ppm mixture was flushed rapidly through the cell for 30 sec, a period long enough for the SO_2 vapor concentration in the cell to reach its maximum value. The gas flow was then stopped abruptly, and the SO_2 vapor concentration was monitored for a few minutes. At one minute after the flow was stopped, the vapor concentration had decreased because of adsorption to 92% of its original value. The concentration continued decreasing and was down to 75% of the original value after 5 minutes. A similar test was performed with a 76 ppm mixture; the rate of percentage decrease was essentially the same as for the leaner mixture.

Another simple test was performed by introducing a 76 ppm mixture into the "clean" sample cell at different flow rates. A constant flow rate of 5 liters per minute was adequate to maintain the SO_2 vapor concentration within less than 1% of the maximum concentration that would be measured with much higher flow rates. The 5 lpm flow rate represents the minimum that can be measured reliably with the low-capacity flowmeter on the manifold assembly. Lower flow rates may be adequate, but if they are used, checks should be made for possible errors due to adsorption.

NOISE LEVEL AND ZERO-DRIFT

The dominant source of noise is the photoelectron noise generated in the photomultiplier. An oscilloscope trace of the photomultiplier output shows no apparent noise during the periods of each cycle when the spinning reticle blocks the uv energy from the photocathode. The noise level, at 30 Hz frequency, on the photomultiplier output was found to be approximately proportional to the square-root of the uv energy level on the photocathode; this relationship is expected when photoelectron noise is dominant. The output of the electronics that process the photomultiplier signal is proportional to the ratio of the 30 Hz component to the 360 Hz component. The 360 Hz component is proportional to the uv energy level on the detector; therefore the 30 Hz noise level on the instrument output is inversely proportional to the square-root of the incident uv energy level. It follows that for a given SO_2 concentration, the signal-to-noise ratio is proportional to the square-root of the incident uv energy level.

The noise level on the 5 ppm full-scale range was measured over a 5-minute interval with no SO_2 in the sample cell, the electronic time constant at 1 sec, and the deuterium arc source operating at 0.7 amps, the maximum current obtainable with the power supply. The output signal was recorded on a strip-chart recorder, and the digital output meter was read once each 5 sec. The peak-to-peak noise level corresponded to approximately 0.2 ppm of SO_2, and the rms noise level as determined from the 60 digital readings was 0.049 ppm. As expected, the noise level decreases when the electronic time constant is increased.

The zero-setting is quite stable, particularly after the instrument has been "warmed-up." During one test period of 30 minutes, the zero-setting, as averaged over a 1-minute interval, drifted less than 0.05 ppm. The amount of zero-drift in practical use will depend mostly on the temperature stability of the air surrounding the instrument.

SAMPLE TURN-OVER TIME

Table 2 sumarizes the results of a series of tests performed to determine the time response of the instrument to an abrupt change in the SO_2 concentration of the gas entering the sample cell. Time resolution, rather than the actual response time, is the quantity of most interest. In a practical application, there is a delay between the time of a sudden change in SO_2 concentration at the exhaust pipe of an automobile and the time that the gas reaches the sample cell where the change is sensed. This delay depends on the gas lines and on the flow rate and will be different for different systems. This delay can be measured and accounted for so that the proper time relationship can be determined between the observed concentration change and any changes in the engine operation.

An important factor in the design of the sample cell and gas-handling system has been the need to maintain good time resolution. Consider the case in which the SO_2 concentration at the inlet to the filter on the pump assembly changes abruptly from level A to a different level B. After a certain delay, the instrument reading starts deviating from level A and goes through a continous change to level B. This period of transition of the instrument reading is a measure of the time resolution, which is a function of gas flow rate, mixing in the sample cell, and electronic response time. The very gradual change in the instrument reading as it approaches level B makes it impractical to measure the complete transition time. In the laboratory tests, we measured times required for 70% and 90% of the change. In every case the period started when there was the first distinct change in the deflection of the recorder that monitored the output signal.

Test No. 1 was performed to determine the response of the recorder to a sudden change in its input signal. The recorder signal was started at approximately 80% of full-scale; the input jack was unplugged suddenly, and the recorder response was measured. This measurement, of course, does not involve the main part of the SO_2 monitor. As in all of the other tests, the recorder chart speed was 1 inch per second. The estimated error in the measured times is approximately 0.05 sec for periods less than 1 sec, and somewhat more for longer periods. The values tabulated represent averages of several independent readings.

Test No. 2 provides information on the response of the electronics, including the photomultiplier, the signal processing electronics and the recorder. The results of this test, or the previous one, have nothing to do with the mixing of the gas in the sample cell. A small mask was held so that it covered a portion of one of the slits of set A in the grid. This produced an output signal that corresponded to approximately 17 ppm of SO_2. While recording the output signal, we abruptly removed the mask. Approximately 0.35 sec was required for the recorder to make 70% of the change; 0.45 sec was required for a 90% change. These times represent the absolute minimum that we would expect to measure when changing the SO_2 concentration if no mixing of the sample took place. The electronic time constant was 0.1 sec for this test and for all tests involving the main electronics.

TABLE 2. RESPONSE TIMES FOR STEP CHANGE IN SO_2 CONCENTRATION AT VARIOUS SAMPLE FLOW RATES

Test No.	Change Made or Flow Rate in lpm	Time for 90% Change (Sec)	Time for 70% Change (Sec)
1	Unplugged Recorder Input Cable	0.29	0.25
2	Uncovered Portion of Grid	0.48	0.35
3	160[a]	0.74	0.45
4	160[b]	0.74	0.48
5	130[b]	0.78	0.55
6	85[b]	1.18	0.73
7	38[b]	1.25	0.88
8	19[b]	1.96	1.43
9	9.5[b]	3.68	2.52

Electronic time constant is 0.1 sec for all tests.

[a]Sample introduced at filter on pump assembly

[b]Sample introduced at distribution tube of sample cell

It is apparent from the results of tests No. 1 and No. 2 that the recorder adds significantly to the measured response times. Somewhat more accurate data on the sample turnover time could be obtained with a faster recorder; however, the lack of a rapid recorder response probably added no more than 0.1-0.2 sec to the times measured when the gas concentration was changed.

Test No. 3 was performed by injecting a slow, steady flow of pure SO_2 into the gas stream just as it entered the filter on the pump assembly. The injection rate of the SO_2 was adjusted to produce a concentration in the line of approximately 17 ppm of SO_2. While recording the output signal, the flow of pure SO_2 was stopped abruptly in such a way that there was no slow diffusion of SO_2 from the injection needle after the flow was stopped. The 70% and 90% turnover times of 0.45 and 0.74 sec indicate that mixing in the gas line and sample cell prevents a gas "front" from moving sharply across the monitoring beam.

Test No. 4 was performed by the same method as Test No. 3, except that the pure SO_2 was injected into the line just ahead of the distribution tube so that it did not travel through the pump and manifold. The results of Tests 3 and 4 are essentially in agreement, indicating that most of the breaking-up of the gas front occurs in the sample cell, not in the pump or manifold assemblies.

Tests 5 through 9 were identical to Test No. 4, except that the sample flow rates were varied. As expected, the turnover times decrease with increasing flow rates, but not in the same proportions. There is apparently less breaking-up of the gas front at low flow rates. For example, in reducing the flow rate by a factor of 9, from 85 lpm to 9.5 lpm, the 90% turnover time increases by a factor of 3.68/1.18 = 3.1. It is apparent that little is gained by operating at flow rates above 130 lpm.

If a much faster recorder were used, the minimum 90% turnover time would probably be between 0.6 and 0.7 sec. This period is somewhat higher than the 0.5 sec design objective.

INTERFERENCE BY OTHER EXHAUST GASES

Interference by automotive exhaust gases other than SO_2 is negligible at the concentrations these gases normally occur in the exhaust. No measurable interference was found for the following hydrocarbons tested individually at Aeronutronic: acetylene, methane, butane, propane, ethylene and ethane. Each sample consisted of a mixture of a single hydrocarbon gas in N_2 at 1 atm total pressure. The data on hydrocarbon interference and other data obtained at Aeronutronic are summarized in Table 3 along with still other data obtained at EPA by EPA scientists.

Many of the interference data were obtained with a small sample cell temporarily placed in the monitoring beam while the main multiple-pass sample cell was by-passed. This improved the signal-to-noise ratio because of the reduction in reflective losses in the multiple-pass optics. The short sample cells also enabled us to use smaller amounts of gas at higher concentrations than would be used in the large, multiple-pass cell. The mixtures of higher concentration are easier to mix accurately, and there is less potential error due to adsorption on the walls of the sample cell. Table 3 gives the cell lengths and the gas concentrations along with the equivalent concentrations for the multiple-pass cell.

Ammonia (NH_3), nitric oxide (NO), and nitrogen dioxide (NO_2) each interfere slightly, but the amount of interference produced by the low concentrations in automotive exhaust is negligible. Because of the detector noise and the very slight interference, the discrimination ratios could not be measured accurately. Nitric oxide absorbs quite strongly in the spectral band employed by the instrument, but there is very little correlation between the structures in the SO_2 spectrum and the NO_2 spectrum. Thus, there is very little interference.

When the 100% CO_2 test gas first entered the sampling volume, the output signal indicated an SO_2 concentration of approximately 0.2 ppm, but this signal vanished as the CO_2 completely displaced the N_2 that was originally in the sample cell. The temporary signal was apparently caused by a non-uniform distribution of the CO_2 in the cell. Differences in the indices of refraction of CO_2 and N_2 probably produce small deflections in the monitoring beam when the gases are both present in the cell and are not mixed. Absorption by CO_2 is completely negligible in the spectral interval passed by the instrument.

A small signal was also observed some of the times when an H_2O mixture first entered the sample cell that was previously filled with N_2. The size of this transient signal was not reproducible, but it never corresponded to more than 0.2 ppm of SO_2. As in the cases when CO_2 was introduced into the cell, the transient signal disappeared when the cell became completely filled with either the H_2O mixture, or with N_2 when the H_2O mixture was being flushed out. When the H_2O mixture was in the sample cell, the 360 Hz component of the detector signal was typically about 1% lower than it was when the cell was filled with N_2. The 1% attenuation is more than can be accounted for by H_2O vapor absorption. This attenuation is not understood, but it may be due to a change in the reflectivity of the mirrors of the multiple-pass optical system that results from a layer of absorbed water on the reflecting surfaces.

The lower part of Table 3 summarizes the results of tests performed on two complex mixtures simulating automobile exhaust hydrocarbons. These mixtures did not contain other common exhaust species such as CO, CO_2, NO_y, or aldehydes such as formaldehyde

The samples were prepared by injecting either gasoline or diesel fuel into a heated tube while purging with nitrogen. The vaporized fuel samples were collected in large Tedlar bags and the total hydrocarbon concentration in ppm determined with a flame ionization detector (F.I.D.) hydrocarbon analyzer. The overall compositions of the two fuels are given as a footnote in Table 3.

The aromatic species in each of these samples would be the most likely to cause interference as they tend to absorb in the U.V. close to the 300nm region which the SO_2 monitor operates. The aromatics in the gasoline are mostly benzene, toluene and other alkyl benzenes. The diesel fuel aromatics contain alkyl benzenes, alkyl naphthalenes, alkyl anthracenes, alkyl phenanthrences and benzothiophenes.

TABLE 3. INTERFERENCE DATA

Test No	Gas	Concentration %	Path Length (cm)	Equiv. Concentration (ppm)	Interference Error (ppm of SO_2)	Discrimination Ratio
1	Acetylene	100	3	6250	N.D.[a]	N.D.
2	Methane	100	3	6250	N.D.	N.D.
3	Butane	100	3	6250	N.D.	N.D.
4	Propane	100	3	6250	N.D.	N.D.
5	Ethylene	100	3	6250	N.D.	N.D.
6	Ethane	100	3	6250	N.D.	N.D.
7	Ammonia	100	3	6250	0.02 [b]	330,000:1
8	Nitrogen-Dioxide	25	0.4	208	0.32 [c]	650:1
9	Nitric Oxide	40	0.4	333	0.01 [d]	30,000:1
10	Carbon Dioxide	100	480	10^6	N.D.	N.D.
11	Water Vapor	2.5	480	25,000	N.D.	N.D.
The following tests on gasoline and diesel fuel were performed at EPA by EPA personnel.						
E1	Gasoline [e]	100 ppm THC	480	100 THC	N.D.	N.D.
E2	Gasoline	400 ppm THC	480	400 THC	N.D.	N.D.
E3	Diesel [e] Fuel	100 ppm THC	480	100 THC	N.D.	N.D.
E4	Diesel Fuel	180 ppm THC	480	180 THC	N.D.	N.D.

(a) N.D. is the abbreviation for Not Detectable

(b) Absorptance of the ammonia sample was 0.02

(c) Absorptance of the NO_2 sample was 0.027

(d) Absorptance of the NO sample was 0.04

(e) The overall compositions of the two fuels were:

	Gasoline	Diesel Fuel
% Paraffins	47.3	82.4
% Olefins	7.8	0.4
% Aromatics	44.9	17.2
	100.0	100.0